Structural Characterization of Edematous Corneas by Forward and Backward Second Harmonic Generation Imaging

Chiu-Mei Hsueh,[†] Wen Lo,[†] Wei-Liang Chen,[†] Vladimir A. Hovhannisyan,[†] Guang-Yu Liu,[†] Sheng-Shun Wang,[†] Hsin-Yuan Tan,[§¶*] and Chen-Yuan Dong[†‡§§*]

[†]Department of Physics and [‡]Center for Quantum Science and Engineering, and [§§]Biomedical Molecular Imaging Core, Division of Genomic Medicine, Research Center for Medical Excellence, National Taiwan University, Taipei, Taiwan; [§]Department of Ophthalmology, Chang Gung Memorial Hospital, College of Medicine, Chang Gung University, Linko, Taiwan; and [¶]Institute of Medical Engineering, College of Medicine and College of Engineering, National Taiwan University, Taipei, Taiwan

ABSTRACT The purpose of this study was to image and quantify the structural changes of corneal edema by second harmonic generation (SHG) microscopy. Bovine cornea was used as an experimental model to characterize structural alterations in edematous corneas. Forward SHG and backward SHG signals were simultaneously collected from normal and edematous bovine corneas to reveal the morphological differences between them. In edematous cornea, both an uneven expansion in the lamellar interspacing and an increased lamellar thickness in the posterior stroma (depth > 200 μm) were identified, whereas the anterior stroma, composed of interwoven collagen architecture, remained unaffected. Our findings of heterogeneous structural alteration at the microscopic scale in edematous corneas suggest that the strength of collagen cross-linking is heterogeneous in the corneal stroma. In addition, we found that qualitative backward SHG collagen fiber imaging and depth-dependent signal decay can be used to detect and diagnose corneal edema. Our work demonstrates that SHG imaging can provide morphological information for the investigation of corneal edema biophysics, and may be applied in the evaluation of advancing corneal edema in vivo.

INTRODUCTION

As the outermost layer of the human vision system, the cornea is responsible for approximately two-thirds of the eye's refractive power (1). Clearly, it is important to maintain corneal transparency for visual clarity. Structurally, type I collagen fibers account for 68% of the dry weight of the cornea (2), and a high degree of corneal transparency depends on the regular ordering of stromal collagen fibrils, which cause destructive interference from scattered light except in the forward direction (3,4). Therefore, any pathological condition that disrupts the collagen fiber alignment can lead to an increase in corneal turbidity (5,6). Normally, the maintenance of corneal transparency is achieved at a constant hydration level of 78%. If the hydration level changes >5% from the normal value, stromal transparency can be adversely affected (7). Physiologically, a number of functions, such as the endothelial pump function and the barrier function of the epithelium and endothelium, contribute to the maintenance of the desired hydration level (8,9). Disruption of these functions can lead to increased hydration in the corneal stroma, resulting in corneal edema. Pathologically, corneal edema can result from various diseases, including endothelial dystrophy, which frequently occurs as a complication from cataract surgery (pseudophakic bullous keratopathy) (10–12). However, it is not clear how the increased fluid content decreases cornea transparency. Therefore, the ability to image and quantify structural alterations in corneal edema may contribute to a better understanding of the underlying biophysics and provide useful information for treating corneal edema in the clinic.

Previous studies investigated corneal edema using techniques such as light and electron microscopy (13), x-ray scattering (14,15), and optical coherence tomography (OCT) (16). Muller et al. (13) compared the architecture of normal and highly hydrated corneas with light microscopy and electron microscopy. Results from electron microscopy indicated that the diameter of the stromal collagen fibers was apparently unaffected. In addition, the interwoven lamellar structure of human anterior stroma (~0–120 μm) was not swollen from the edematous condition. Besides, x-ray scattering studies in swollen, ex vivo human corneas revealed no significant changes in collagen fibril diameter throughout the tissue, and smaller interfibrillar spacing of collagen was found in the anterior-most regions of the stroma (14). Furthermore, an x-ray study showed that, at or above the physiological hydration level of stroma, partially imbibed water associated with stromal swelling keeps fibrils apart and results in irregular extrafibrillar spacing (15). Finally, OCT results showed a significant increase in backscattered light from the posterior stroma of edematous human cornea, and it was proposed that the increased scattering came primarily from localized hydration and a mismatched refractive index (16). Specifically, localized hydration associated with the imbibed water distribution would cause an alteration in the stromal structure and change the refractive index ratio of collagen fibrils and extrafibrillar matrix, resulting in scattering (17–20).

Although corneal edema has been well studied, there are limitations associated with the techniques used. The sample

Submitted August 27, 2008, and accepted for publication May 4, 2009.

*Correspondence: d93548010@ntu.edu.tw or cydong@phys.ntu.edu.tw

Editor: Alberto Diaspro.

0006-3495/09/08/1198/8 $2.00

doi: 10.1016/j.bpj.2009.05.040

preparation procedures associated with histological examination and electron microscopy may cause the loss or inaccuracy of the structural information. Furthermore, x-ray diffraction and OCT cannot resolve detailed and individualized structural information of individual collagen fibrils. In addition, the transparency of cornea hinders the direct observation of corneal structure by standard optical microscopy. Finally, a quantitative metric characterizing collagen structural alteration with minimal tissue disturbance is lacking. The demonstration of a minimally invasive, high-resolution imaging modality that could provide both morphological and quantitative information regarding structural alterations in corneal edema would facilitate the study of corneal biophysics and enable the development of a clinically diagnostic tool for this pathology. Since the corneal stroma is composed primarily of type I collagen that is capable of emitting strong second harmonic generation (SHG) signals, SHG microscopy may be useful for addressing issues associated with corneal edema that are not accessible by other imaging modalities.

SHG microscopy uses the nonlinear excitation from ultrafast, near-infrared laser sources and has the advantage of enhanced penetrating depth. It can be used to achieve label-free imaging of noncentrosymmetric biological tissues with minimal invasiveness (21). Previously, multiphoton autofluorescence and SHG microscopy were applied to image the three-dimensional (3D) structure of ex vivo cornea (22). For imaging corneal pathologies, multiphoton microscopy has been shown to be successful in detailing morphological changes in conditions such as infectious keratitis, keratoconus, conductive keratoplasty-induced wound healing, and changes in the optic nerve head (23–27). In this work, we used SHG microscopy to image and quantify structural alterations in edematous and untreated bovine corneas.

MATERIALS AND METHODS

SHG microscope

The schematic of the multiphoton imaging system used in this study is shown in Fig. 1. Our multiphoton microscope was built in-house and is based on a commercial upright microscope (E800; Nikon, Tokyo, Japan). The excitation source is a titanium-sapphire (ti-sa) laser (Tsunami; Spectra Physics, Mountain View, CA) pumped by a diode-pumped, solid-state laser system (Millennia X; Spectra Physics). The 780 nm output of the ti-sa laser was used for sample excitation, and the images were acquired using a water immersion objective (S Flour, 40×, NA 0.8, WI; Nikon). The nominal laser pulse duration was ~100 fs, and the repetition rate was 80 MHz. The laser power used was ~96 mW and 139 mW (at the sample) for normal and edematous corneas, respectively. No photodamage or SHG signal saturation was observed. Higher power on edematous cornea was used to compensate for the weaker signal detected from greater imaging depths caused by increased scattering. In this study, we gathered both the forward SHG (FWSHG) and backward SHG (BWSHG) signals simultaneously. In the backward collection geometry, BWSHG signals were collected by the focusing objective. After the signals passed through a short-pass dichroic mirror (700dcspruv3p; Chroma Technology, Rockingham, VT), they were separated by the secondary dichroic mirror (435 dcxr; Chroma Technology) and filtered by band-pass filters (HQ390/20; Chroma Technology) for the collection of BWSHG signals (380–400 nm). In the forward mode, FWSHG signals were collected by a lens with 50 mm focal length and passed through a band-pass filter (HQ390/20; Chroma Technology) before they were detected. In both the forward and backward signal collections, single photon counting photomultipliers (R7400P; Hamamatsu, Hamamatsu, Japan) were used. To obtain images with both high resolution and large-scale features in three dimensions, we adapted a motorized translational stage (H101; Prior Scientific Instrument, Cambridge, UK) to the microscope for specimen translation after each optical image (256 × 256 pixels) was acquired.

Sample preparation

The bovine eyes used in this experiment were obtained from a local market on the morning of the experiment. Corneal buttons ~7 mm in diameter were excised from the center of the cornea following routine sterilization procedures. In the normal group, the corneal buttons were wrapped with Kimwipes tissue paper soaked with phosphate-buffered saline solution and placed in the glass bottom culture dish for observation. For the edematous group, the

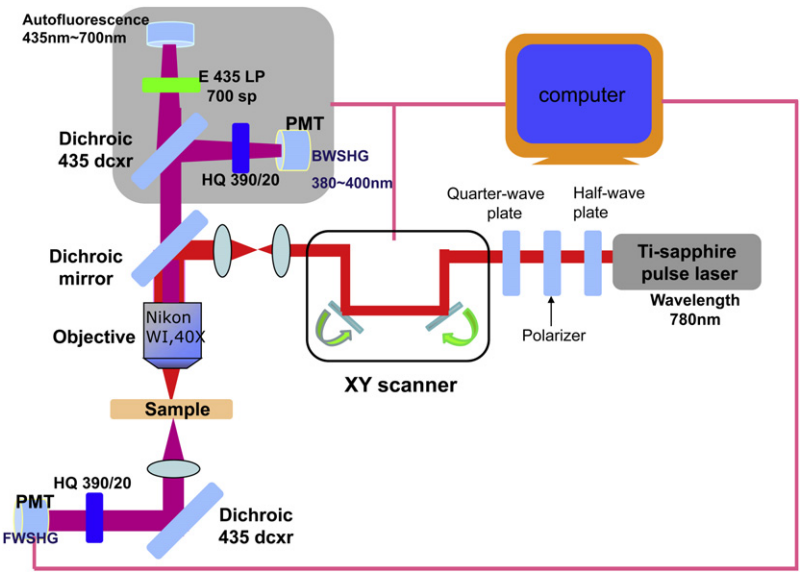

FIGURE 1 Experimental setup of the SHG microscope.

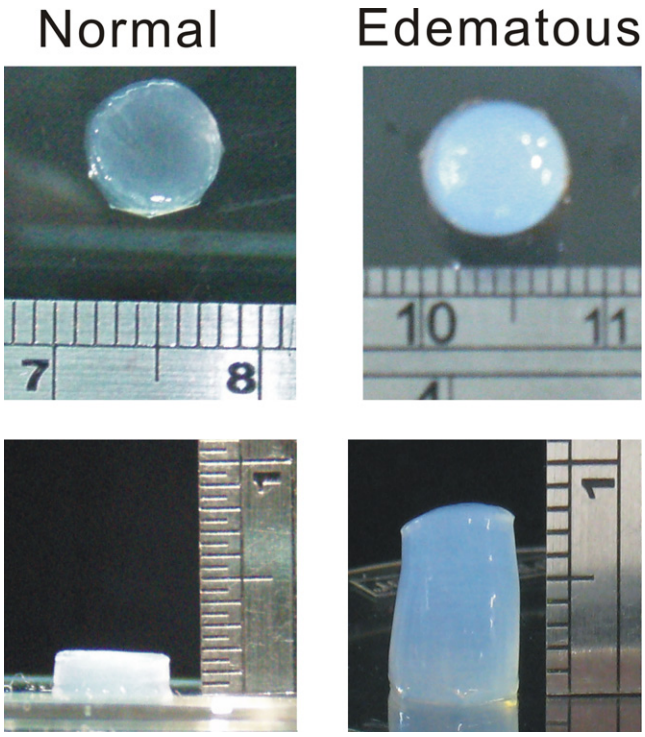

FIGURE 2 Photographs of normal and edematous corneas. En face (*top*) and side (*bottom*) views are shown.

corneal buttons were immersed in deionized water for 2 h to induce corneal edema. Although others have used longer induction times, we found that 2 h were sufficient to induce significant edema in the treated corneas (13).

Shown in Fig. 2 are the representative en face and side views of normal and edematous corneas. The en face photos show that the normal and edematous corneas are comparable in diameter. However, in comparison with a normal cornea, the side view of the edematous corneal button shows a significant increase in thickness. This observation suggests that the overhydrated cornea has a much higher tendency to expand in the axial direction. Furthermore, note that the edematous corneas are more opaque in the en face images, but are more transparent when viewed from the side. The en face observation is understandable since hydration is expected to disrupt the interference process that is responsible for normal corneal clarity (3). However, from the side view, the interference condition for corneal transparency in the en face direction does not hold. Therefore, the increased fluid content is expected to contribute to greater optical clarity.

The bovine corneal buttons of these two groups were placed on a glass bottom culture dish (Part No. P50G-1.5-14-F; MatTek, Ashland, MA) and then covered with coverglasses (No. 990; Mikroskopische Deckglaser, Karl Hecht KG Assistent, Sondheim, Germany) to maintain corneal moisture. Each corneal button was imaged in the direction from the anterior to the posterior stroma (forward direction), and imaged again in the direction from the posterior to the anterior stroma (reverse direction) by inverting the culture dish.

Measurement of lamella thickness

In addition to qualitative FWSHG and BWSHG imaging, we also measured lamella thickness under edematous conditions. Since a stromal lamellar layer is composed of long, parallel collagen fibrils (28), the lamella thickness can be determined from the FWSHG images by measuring the axial positions at which a collagen fibril with a given orientation was observed. In our measurement, each area chosen for analysis was 3×3 pixels in size (1.29×1.29 μm^2), and only the collagen fibril that appeared in this area was analyzed. This method is illustrated in Fig. 3 for a normal bovine cornea. For each corneal button, three randomly chosen areas were analyzed to determine the lamella thickness at different depths, and the average lamella thickness was determined along the axial direction at 200 μm increments. *T*-test was used to determine whether there were statistical differences in the lamellar thickness between normal and edematous corneas in both the anterior and posterior regions.

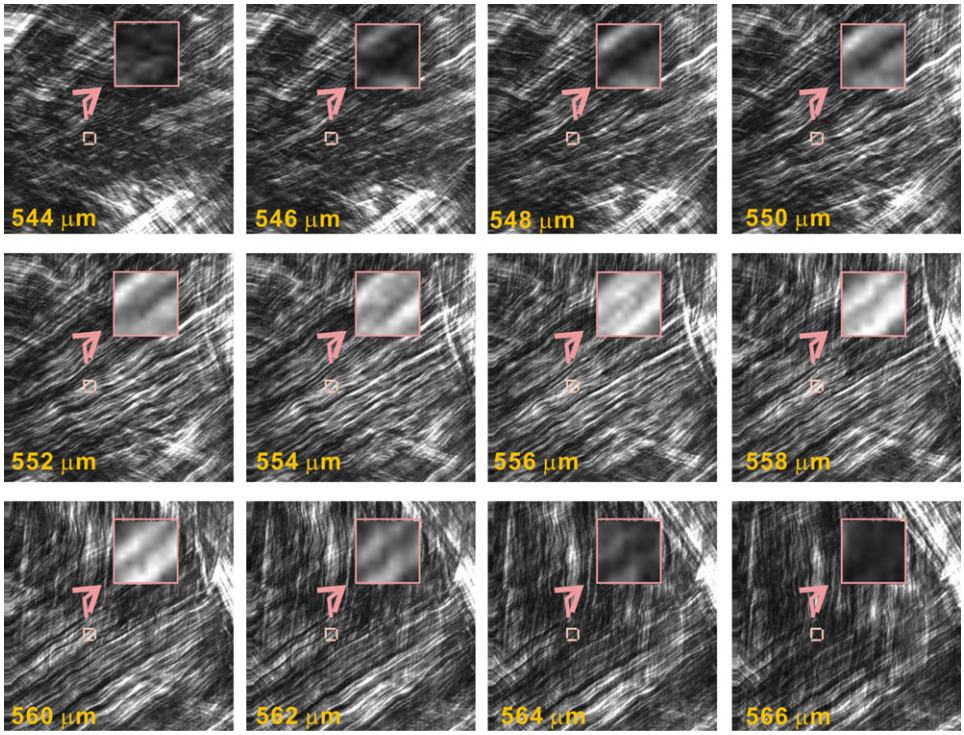

FIGURE 3 Demonstration of the lamella thickness measurement method using en face FWSHG images of normal bovine cornea at different depths. The first to last images show the appearance and disappearance of collagen fibril with a given orientation.

RESULTS AND DISCUSSION

To reveal the details of cornea edema under SHG imaging, en face FWSHG images of the stroma were acquired (Fig. 4). As the images show, stromal collagen fibers are structurally distinct in a depth-dependent manner. At a depth of 100 μm, the tightly interwoven collagen fibers were observed in the FWSHG images of both the normal and edematous corneas. At a depth of 1000 μm, the FWSHG images of the normal and edematous corneas show that the collagen fibrils are mutually parallel in forming the lamella. Moreover, morphological features from the en face FWSHG images show that the edematous cornea has structural details similar to those found in the normal cornea. Furthermore, with increasing imaging depth, the BWSHG image of the edematous cornea becomes similar in appearance to the FWSHG images in revealing the fibrous morphology of stromal collagen.

Series of FWSHG and BWSHG images collected along the axial direction were reconstructed three-dimensionally to investigate the lamella structure alteration (Fig. 5). Stacks of both FWSHG and BWSHG images with a total thickness of 1000 μm, at 2 μm steps, were obtained from both anterior–posterior and posterior–anterior directions in normal and edematous groups (Fig. 5, *A–H*). From the 3D reconstruction of the FWSHG images in normal and edematous corneas, it can be seen that the stroma is composed of lamella stacks (Fig. 5, *A*, *C*, *E*, and *G*). Specifically, Fig. 5, *A* and *E*, show that the normal corneal stroma lamellae are parallel to the surface of the cornea. Nonetheless, the interlacing lamellae structure was observed near the cornea bottom, which is consistent with the interlacing lamella structure performed by SEM (29). Furthermore, the BWSHG images (Fig. 5, *B* and *F*) of the normal cornea are morphologically different from the FWSHG images. However, in some cases, a lamellae structure similar to the FWSHG result can be obtained from the BWSHG images (29). In the edematous group, the FWSHG (Fig. 5, *C* and *G*) and BWSHG (Fig. 5, *D* and *H*) images are morphologically similar, as both reveal the lamellar architecture of stromal collagen. However, it was observed that some lamellae were oblique to the corneal surface (*arrow* in Fig. 5 *D*). To further quantify this result, we measured the inclination angles of collagen fibers relative to the horizontal axis between normal and edematous corneas at positions I, II, III, and IV. It was found that the inclination angles in normal cornea were ~10° (I) to 17° (II), much smaller than those in edematous cornea (28° (III) or 27° (IV)). In addition, regions void of SHG signals were found between adjacent lamellae and were likely filled with imbibed water (*arrowhead* in Fig. 5 *H*). These observations support the notion that structural modifications (e.g., increases in lamellae spacing) in corneal edema occur nonuniformly throughout the stroma. Therefore, our findings suggest that the imbibed fluid is not distributed evenly among lamellae within edematous stroma.

To further characterize morphological changes in edematous corneas, detailed images at different depths in Fig. 5, *A–D*, are shown in Fig. 6. The depth-resolved FWSHG images reveal the irregularly interwoven collagen fibril sheet in the anterior stroma. This observation is consistent with results from transmission electron microscopy and scanning electron microscopy (28,30). Furthermore, we noticed that the stroma collagen structure changed from the interwoven architecture to lamellar stacks beyond 200 μm in both normal and edematous corneas. We also found that the normalized BWSHG and FWSHG signals decayed significantly with increasing depths, especially beyond the depth of 200 μm (Fig. 7). Furthermore, we observed that the axial SHG intensity profiles displayed a larger degree of fluctuation in normal than in edematous corneas. This may be due to the fact that the structural heterogeneity that contributes to the SHG intensity variation is further stretched when the corneas become overhydrated. The observation of different SHG intensity decay rates is consistent with increased opacity (stronger scattering) in the swollen corneas (Fig. 2). Therefore, the nominal depth of 200 μm can be considered to be the boundary separating domains of bovine corneas that are differently affected by corneal edema. In addition, note that with increasing depths, the SHG images of edematous corneas degrade more significantly than the normal corneal images. Two factors likely contribute to

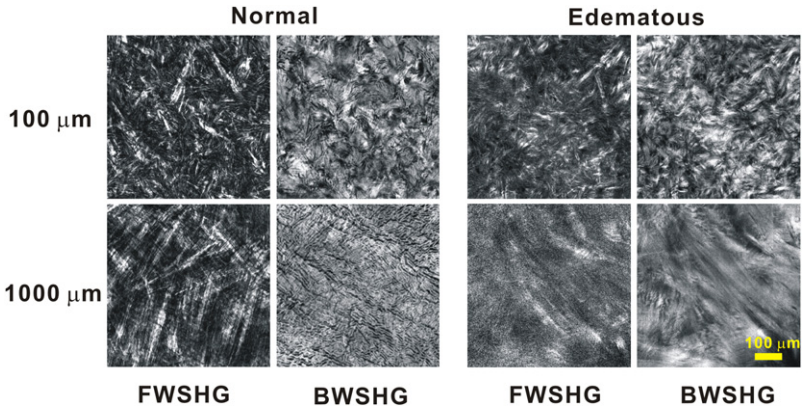

FIGURE 4 Large-area morphological comparison in the *x-y* plane between normal and edematous bovine corneas at depths of 100 μm (*top*) and 1000 μm (*bottom*) measured in the anterior–posterior direction.

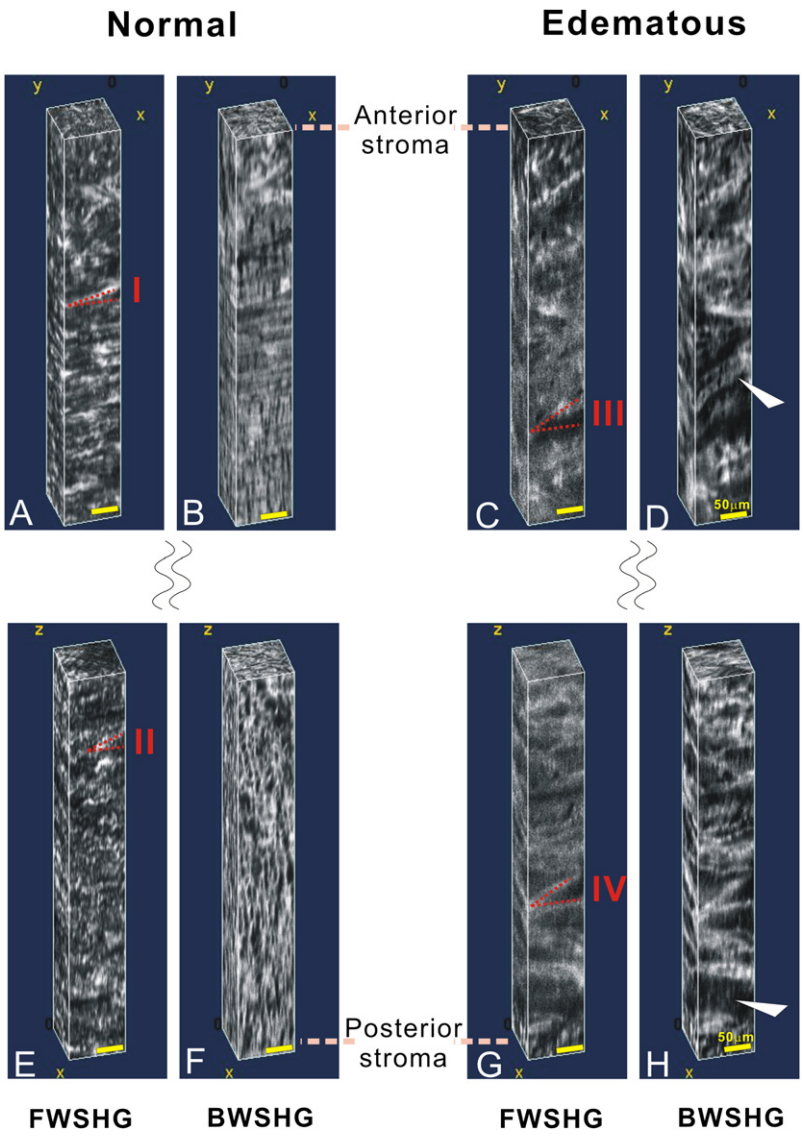

FIGURE 5 Stacks of FWSHG and BWSHG images with a total thickness of 1000 μm from both the anterior–posterior and posterior–anterior directions in the normal (*A*, *B*, *E*, and *F*) and edematous (*C*, *D*, *G*, and *H*) groups.

this phenomenon. First, the increased scattering in edematous corneas can degrade both the detectable FWSHG and BWSHG signals. Second, in BWSHG imaging, the increase in the backscattered component of the FWSHG signal from opaque edematous corneas may interfere with the inherent BWSHG signal.

We also determined lamella thickness in normal and edematous corneas (Fig. 8). In the anterior stroma (0~200 μm), the lamella thickness was 23 μm on average and was not statistically different between the normal and edematous groups ($p > 0.05$). Furthermore, the lamellar thickness in normal corneas did not change significantly beyond 200 μm. However, for the edematous corneas, the average lamella thickness increased to the 30–45 μm range at depths > 200 μm ($p < 0.05$). Our observation that the anterior stroma was less affected by swelling is consistent with a previous x-ray study (13). On occasion, lamellar layers with extensive expansion (~60 or 70 μm) were found beyond the depth of 200 μm in edematous corneas. Our finding suggests that the swollen lamella extended nonuniformly in the stroma. Most likely, the interwoven architecture of the anterior stroma leads to a resistance to swelling (31), and additional proteoglycan in the posterior stroma may also affect the swelling behavior (32–35).

In addition, we found that the overall increase in corneal thickness was disproportional to the degree of lamellar expansion. To be specific, the thickness of edematous cornea increased ~3-fold, whereas the lamella thickness increased by a factor of ~1.5. This observation suggests that the imbibed water spread not only in interlamellar space but also in intralamellar space, which is also consistent with Meek et al.'s (36) result. Specifically, we found that more water was imbibed in interlamellar space, corresponding to the dark regions shown in Fig. 5.

Since collagen fibrils are most likely the primary cause of scattering in corneal stroma (37), the structural changes in

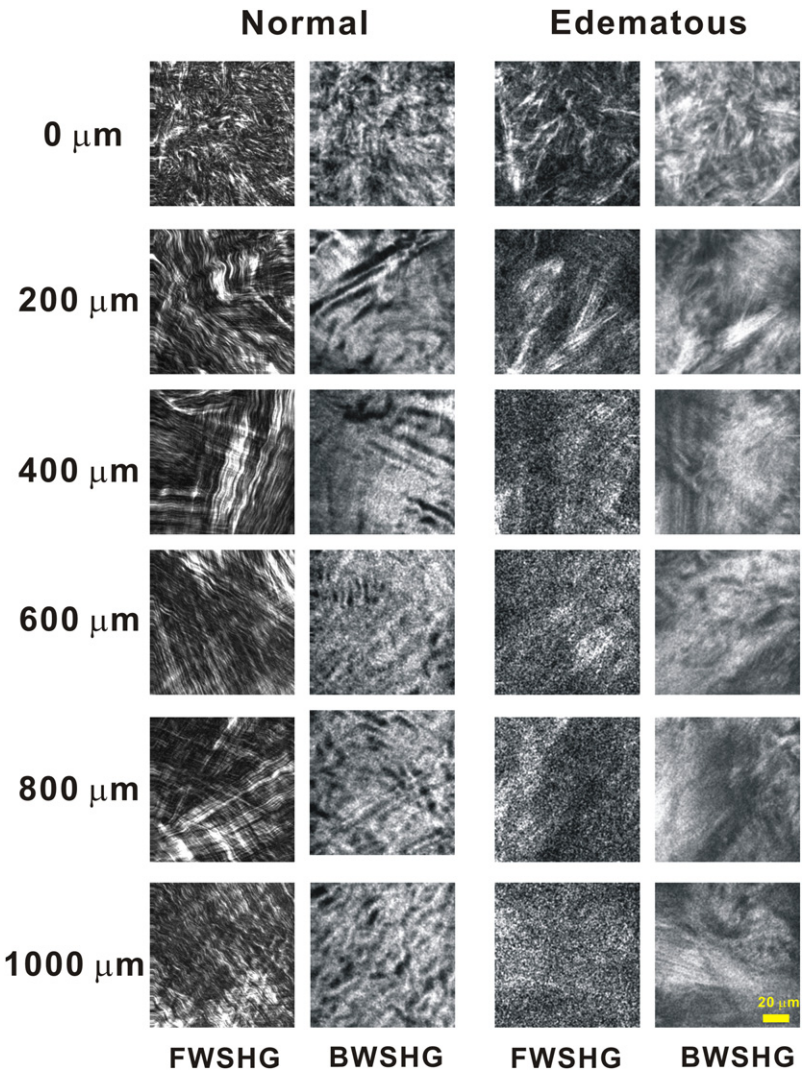

FIGURE 6 Depth-resolved en face SHG images of an image stack from Fig. 5, *A–D*, respectively.

edematous corneas probably contributed to the differences between our BWSHG and FWSHG results. Specifically, when corneas swell, changes in the relative refractive index between the extrafibrillar spacing and collagen fibrils, combined with increased interlamellar space, can contribute to increased scattering (19). Furthermore, it is possible that collagen fibers with altered orientation (oblique lamellae in Fig. 5) can also contribute to scattering. Our study shows that the distortion of the collagen fibrillar spatial arrangement and the irregular distribution of fibril-free regions between lamella layers are likely contributors to increased corneal turbidity and enhanced backscattering of the FWSHG signal.

CONCLUSIONS

In this study, SHG imaging was used to visualize the structural lamellar organization of edematous cornea at micron resolution, and the results demonstrate the potential of this technique for providing structural information on edematous cornea. We found that the increased intralamellar spacing in the edematous cornea group and the associated increase in lamella thickness occurred primarily in the posterior stroma. In the anterior region (<200 μm), the strongly cross-linked and more tightly interwoven collagen matrix offers mechanical resistance to lamellar expansion from hydration. Our results also show that qualitative BWSHG imaging and depth-dependent signal decay can be used to detect and diagnose corneal edema. Specifically, BWSHG images of edematous corneas show a fibrous architecture of collagen fibers similar to that found in FWSHG images. Finally, our findings of heterogeneous structural alteration in edematous corneas suggest that the strength of collagen cross-linking is heterogeneous in the corneal stroma. Due to its minimally invasive nature, SHG imaging can be used to study the underlying biophysics of corneal edema. It can reveal morphological features and facilitate quantitative analysis to help evaluate the necessity for full- or partial-thickness corneal transplantation in corneal edema cases. With additional development, SHG microscopy may become a clinically diagnostic tool for corneal edema.

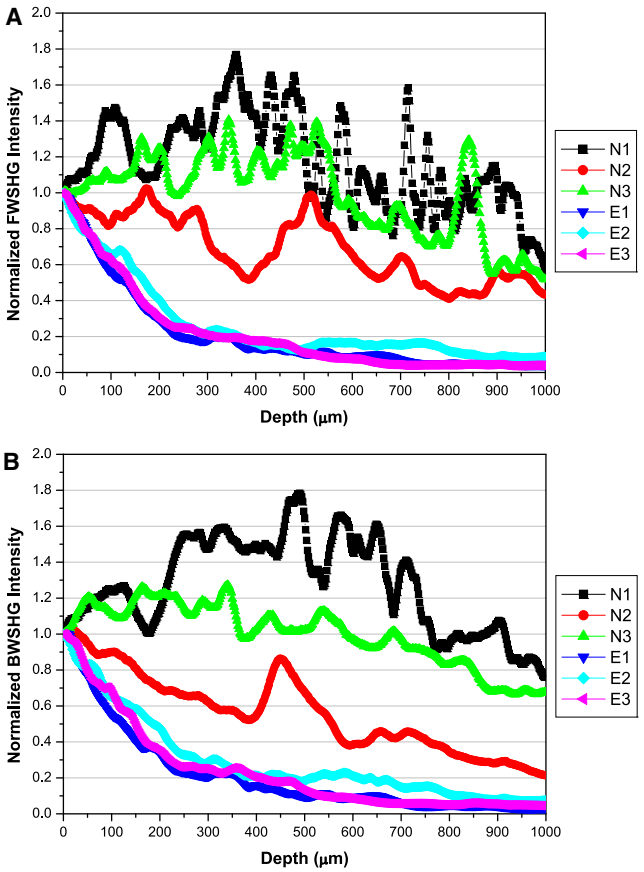

FIGURE 7 Depth dependence of normalized FWSHG (*A*) and BWSHG (*B*) intensities in three different normal (N1, N2, and N3) and edematous (E1, E2, and E3) corneas in the anterior–posterior direction.

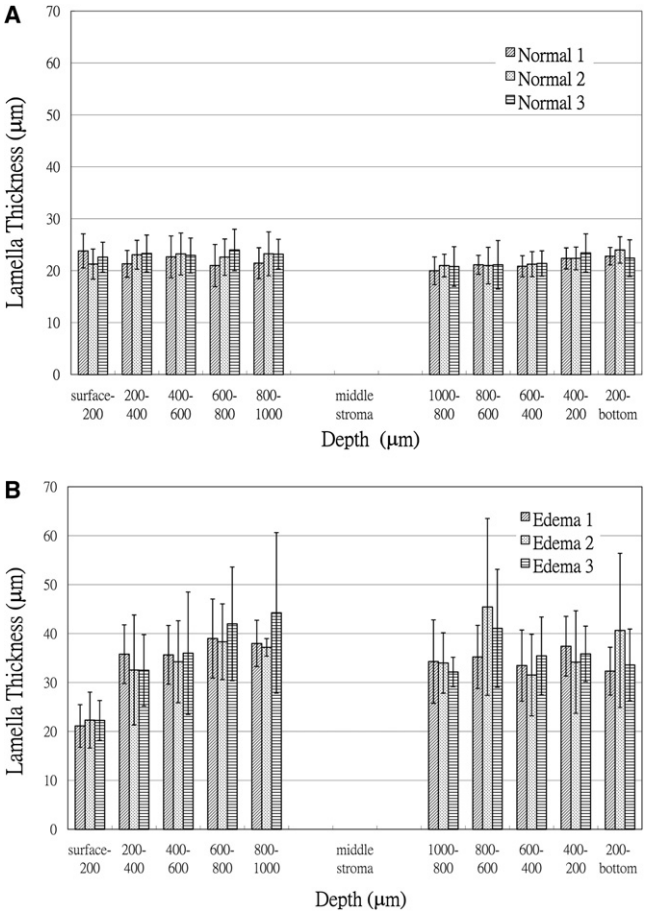

FIGURE 8 Histograms of the depth-dependent, corneal lamella thickness (mean ± SD) comparison between normal (*A*) and edematous (*B*) corneas.

This study was supported by the National Research Program of Genomic Medicine, National Science Council, Taiwan. The work was completed in the Optical Molecular Imaging Microscopy Core Facility (A5) of the National Research Program of Genomic Medicine.

REFERENCES

1. Forrester, J. V. 2002. The Eye: Basic Sciences in Practice. W.B. Saunders, Edinburgh/New York.
2. Maurice, D. M. 1984. The cornea and sclera. *Eye*. 1:103–115.
3. Maurice, D. M. 1957. The structure and transparency of the cornea. *J. Physiol.* 136:263–286.
4. Hart, R. W., and R. A. Farrell. 1969. Light scattering in the cornea. *J. Opt. Soc. Am.* 59:766–774.
5. Freund, D. E., R. L. McCally, and R. A. Farrell. 1986. Effects of fibril orientations on light scattering in the cornea. *J. Opt. Soc. Am. A.* 3:1970–1982.
6. Farrell, R. A., R. L. McCally, and P. E. Tatham. 1973. Wave-length dependencies of light scattering in normal and cold swollen rabbit corneas and their structural implications. *J. Physiol.* 233:589–612.
7. Hodson, S. A. 1997. Corneal stromal swelling. *Prog. Retin. Eye Res.* 16:99–116.
8. Harris, J. E. 1962. Symposium on the cornea. Introduction: factors influencing corneal hydration. *Invest. Ophthalmol.* 1:151–157.
9. Maurice, D. M. 1972. The location of the fluid pump in the cornea. *J. Physiol.* 221:43–54.
10. Holden, B. A., K. A. Polse, D. Fonn, and G. W. Mertz. 1982. Effects of cataract surgery on corneal function. *Invest. Ophthalmol. Vis. Sci.* 22:343–350.
11. Schultz, R. O., D. B. Glasser, M. Matsuda, R. W. Yee, and H. F. Edelhauser. 1986. Response of the corneal endothelium to cataract surgery. *Arch. Ophthalmol.* 104:1164–1169.
12. Ventura, A. C., R. Walti, and M. Bohnke. 2001. Corneal thickness and endothelial density before and after cataract surgery. *Br. J. Ophthalmol.* 85:18–20.
13. Müller, L. J., E. Pels, and G. Vrensen. 2001. The specific architecture of the anterior stroma accounts for maintenance of corneal curvature. *Br. J. Ophthalmol.* 85:437–443.
14. Quantock, A. J., C. Boote, R. D. Young, S. Hayes, H. Tanioka, et al. 2007. Small-angle fibre diffraction studies of corneal matrix structure: a depth-profiled investigation of the human eye-bank cornea. *J. Appl. Cryst.* 40:335–340.
15. Meek, K. M., N. J. Fullwood, P. H. Cooke, G. F. Elliott, D. M. Maurice, et al. 1991. Synchrotron x-ray diffraction studies of the cornea, with implications for stromal hydration. *Biophys. J.* 60:467–474.
16. Wang, J., T. L. Simpson, and D. Fonn. 2004. Objective measurements of corneal light-backscatter during corneal swelling, by optical coherence tomography. *Invest. Ophthalmol. Vis. Sci.* 45:3493–3498.
17. Meek, K. M., and N. J. Fullwood. 2001. Corneal and scleral collagens—a microscopist's perspective. *Micron.* 32:261–272.

18. Kim, Y. L., J. T. Walsh, Jr., T. K. Goldstick, and M. R. Glucksberg. 2004. Variation of corneal refractive index with hydration. *Phys. Med. Biol.* 49:859–868.

19. Meek, K. M., S. Dennis, and S. Khan. 2003. Changes in the refractive index of the stroma and its extrafibrillar matrix when the cornea swells. *Biophys. J.* 85:2205–2212.

20. Leonard, D. W., and K. M. Meek. 1997. Refractive indices of the collagen fibrils and extrafibrillar material of the corneal stroma. *Biophys. J.* 72:1382–1387.

21. Sun, C. K., S. W. Chu, S. Y. Chen, T. H. Tsai, T. M. Liu, et al. 2004. Higher harmonic generation microscopy for developmental biology. *J. Struct. Biol.* 147:19–30.

22. Teng, S. W., H. Y. Tan, J. L. Peng, H. H. Lin, K. H. Kim, et al. 2006. Multiphoton autofluorescence and second-harmonic generation imaging of the ex vivo porcine eye. *Invest. Ophthalmol. Vis. Sci.* 47:1216–1224.

23. Morishige, N., A. J. Wahlert, M. C. Kenney, D. J. Brown, K. Kawamoto, et al. 2007. Second-harmonic imaging microscopy of normal human and keratoconus cornea. *Invest. Ophthalmol. Vis. Sci.* 48:1087–1094.

24. Yeh, A. T., N. Nassif, A. Zoumi, and B. J. Tromberg. 2002. Selective corneal imaging using combined second-harmonic generation and two-photon excited fluorescence. *Opt. Lett.* 27:2082–2084.

25. Tan, H. Y., Y. Sun, W. Lo, S. J. Lin, C. H. Hsiao, et al. 2006. Multiphoton fluorescence and second harmonic generation imaging of the structural alterations in keratoconus ex vivo. *Invest. Ophthalmol. Vis. Sci.* 47:5251–5259.

26. Wang, T. J., W. Lo, C. M. Hsueh, M. S. Hsieh, C. Y. Dong, et al. 2008. Ex vivo multiphoton analysis of rabbit corneal wound healing following conductive keratoplasty. *J. Biomed. Opt.* 13:034019.

27. Brown, D. J., N. Morishige, A. Neekhra, D. S. Minckler, and J. V. Jester. 2007. Application of second harmonic imaging microscopy to assess structural changes in optic nerve head structure ex vivo. *J. Biomed. Opt.* 12:024029.

28. Komai, Y., and T. Ushiki. 1991. The three-dimensional organization of collagen fibrils in the human cornea and sclera. *Invest. Ophthalmol. Vis. Sci.* 32:2244–2258.

29. Radner, W., and R. Mallinger. 2002. Interlacing of collagen lamellae in the midstroma of the human cornea. *Cornea.* 21:598–601.

30. Muller, L. J., E. Pels, L. Schurmans, and G. Vrensen. 2004. A new three-dimensional model of the organization of proteoglycans and collagen fibrils in the human corneal stroma. *Exp. Eye Res.* 78:493–501.

31. Bron, A. J. 2001. The architecture of the corneal stroma. *Br. J. Ophthalmol.* 85:379–381.

32. Boote, C., S. Dennis, Y. Huang, A. J. Quantock, and K. M. Meek. 2005. Lamellar orientation in human cornea in relation to mechanical properties. *J. Struct. Biol.* 149:1–6.

33. Huang, Y., and K. M. Meek. 1999. Swelling studies on the cornea and sclera: the effects of pH and ionic strength. *Biophys. J.* 77:1655–1665.

34. Castoro, J. A., A. A. Bettelheim, and F. A. Bettelheim. 1988. Water gradients across bovine cornea. *Invest. Ophthalmol. Vis. Sci.* 29:963–968.

35. Lee, D., and G. Wilson. 1981. Non-uniform swelling properties of the corneal stroma. *Curr. Eye Res.* 1:457–461.

36. Meek, K. M., D. W. Leonard, C. J. Connon, S. Dennis, and S. Khan. 2003. Transparency, swelling and scarring in the corneal stroma. *Eye.* 17:927–936.

37. Richards-Kortum, R., and E. Sevick-Muraca. 1996. Quantitative optical spectroscopy for tissue diagnosis. *Annu. Rev. Phys. Chem.* 47:555–606.